Deep-Sea Research I 91 (2014) 115–124

Contents lists available at ScienceDirect

Deep-Sea Research I

journal homepage: www.elsevier.com/locate/dsri

Seasonal changes in zooplankton abundance, biomass, size structure and dominant copepods in the Oyashio region analysed by an optical plankton counter

Atsushi Yamaguchi *, Kohei Matsuno, Yoshiyuki Abe, Daichi Arima, Kohei Ohgi

Laboratory of Marine Biology, Graduate School of Fisheries Sciences, Hokkaido University, 3-1-1 Minatomachi, Hakodate, Hokkaido 041-8611, Japan

ARTICLE INFO

Article history:
Received 23 January 2013
Received in revised form
4 June 2014
Accepted 13 June 2014
Available online 23 June 2014

Keywords:
Eucalanus
Metridia
Neocalanus
ESD
Life cycle
OPC

ABSTRACT

To identify seasonal patterns of change in zooplankton communities, an optical plankton counter (OPC) and microscopic analysis were utilised to characterise zooplankton samples collected from 0 to 150 m and 0 to 500 m in the Oyashio region every one to three months from 2002 to 2007. Based on the OPC measurements, the abundance and biomass of zooplankton peaked in June (0–150 m) or August (150–500 m), depending on the depth stratum. The peak periods of the copepod species that were dominant in terms of abundance and biomass indicated species-specific patterns. Three *Neocalanus* species (*Neocalanus cristatus*, *Neocalanus flemingeri* and *Neocalanus plumchrus*) exhibited abundance peaks that occurred before their biomass peaks, whereas *Eucalanus bungii* and *Metridia pacifica* experienced biomass peaks before their abundance peaks. The abundance peaks corresponded to the recruitment periods of early copepodid stages, whereas the biomass peaks corresponded to the periods when the dominant populations reached the late copepodid stages (C5 or C6). Because the reproduction of *Neocalanus* spp. occurred in the deep layer (> 500 m), their biomass peaks were observed when the major populations reached stage C5 after the abundance peaks of the early copepodid stages. The reproduction of *E. bungii* and *M. pacifica* occurred near the surface layer. These species first formed biomass peaks of C6 and later developed abundance peaks of newly recruited early copepodid stages. From the comparison between OPC measurements and microscopic analyses, seasonal changes in zooplankton biomass at depths of 0–150 m were governed primarily by *E. bungii* and *M. pacifica*, whereas those at depths of 150–500 m were primarily caused by the three *Neocalanus* species.

1. Introduction

The Oyashio region is located in the western subarctic Pacific and is influenced by the Oyashio Current, which mixes with the colder, less saline water of the Okhotsk Sea on its way southwest from the Kurile Islands (Kono, 1997). The Oyashio region is sometimes covered with warm-core rings from the Kuroshio Current (Yasuda et al., 1992; Kono, 1997). Seasonal changes in the Oyashio pelagic ecosystem are characterised by a massive phytoplankton bloom in spring and a subsequent increase in zooplankton biomass (Kasai et al., 1997, 2001; Saito et al., 2002). The zooplankton biomass in this region is dominated by large grazing copepods (*Neocalanus* spp., *Eucalanus bungii* and *Metridia pacifica*) (73% of total zooplankton biomass, cf. Ikeda et al., 2008). Information on the life cycle patterns of these copepods has accumulated rapidly during the past decade (Kobari and Ikeda, 1999, 2001a, 2001b; Tsuda et al., 1999, 2004). However, information on whole zooplankton communities, especially seasonal changes in their sizes, is scarce.

From the viewpoint of fisheries, the prey size of pelagic fishes is known to vary with ontogeny (Oozeki et al., 2004). Information on zooplankton size composition is important because it affects fish energy costs and growth and mortality rates (van der Meeren and Næss, 1993; Yamamura, 2004) and regulates the vertical particulate flux through the biological pump (Boyd and Newton, 1999; Ducklow et al., 2001). Little information is available on the size composition of zooplankton in the Oyashio region. This is partly because evaluating size for zooplankton samples via ordinary microscopic analysis is very time-consuming. To overcome this problem, analysis of zooplankton samples using an Optical Plankton Counter (OPC) (Herman, 1988, 1992; Beaulieu et al., 1999) can provide accurate sizes and numbers of zooplankton much more quickly than microscopic analysis.

In this study, we performed an OPC analysis on preserved zooplankton samples collected from 0 to 150 m and 0 to 500 m in

* Corresponding author. Tel/fax: +81 138 40 5631.
E-mail address: a-yama@fish.hokudai.ac.jp (A. Yamaguchi).

http://dx.doi.org/10.1016/j.dsr.2014.06.003
0967-0637/

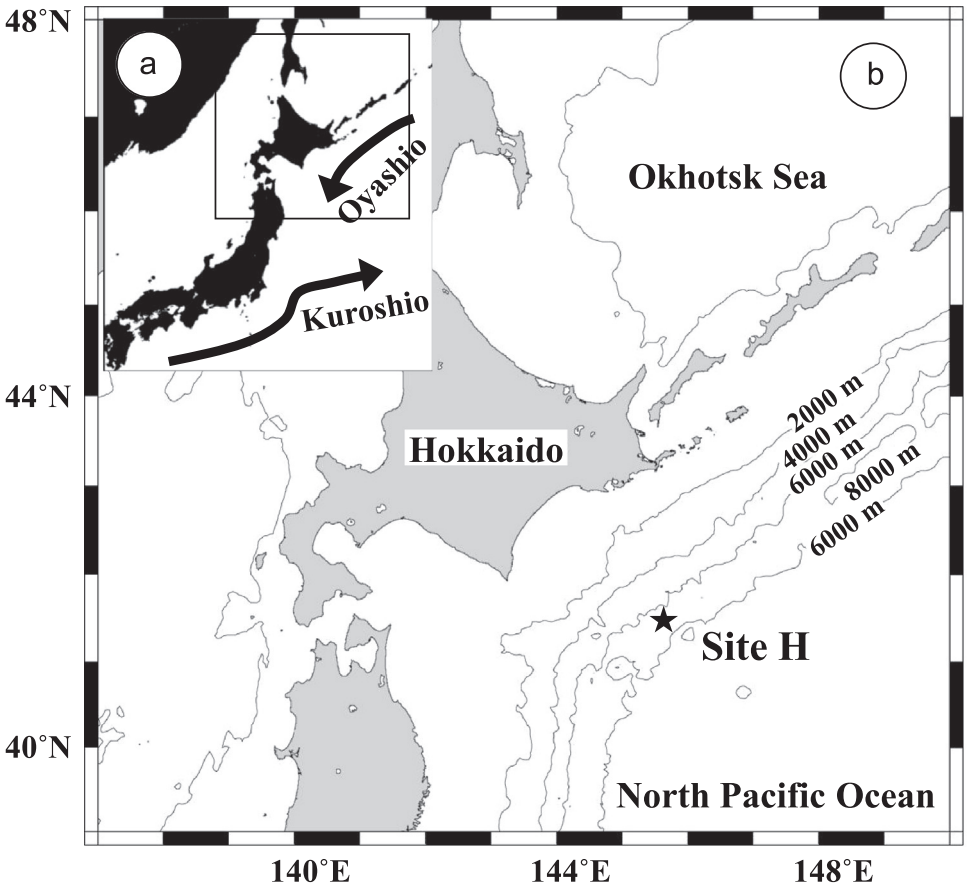

Fig. 1. Location of the Oyashio region in the western subarctic Pacific (a) and of sampling station Site H in the Oyashio region (b).

the Oyashio region every one to three months from 2002 to 2007 (six years). Large grazing copepod species (*Neocalanus* spp., *E. bungii* and *M. pacifica*) were identified, classified by stage, and counted. Based on these copepod data, we also evaluated the seasonal pattern of change in the species composition of the dominant copepods within the 0–500 m stratum of the Oyashio region. Finally, knowing the size of each copepodid stage, we were able to estimate the copepod species composition of the zooplankton biomass based on its size distribution, and we determined which species govern seasonal changes in the zooplankton biomass within the Oyashio region.

2. Material and methods

2.1. Zooplankton sampling

Zooplankton samples were collected with twin NORPAC nets (0.335 mm and 0.100 mm mesh (Motoda, 1957)), at Site H (41°30′N, 145°47′E, Fig. 1) in the Oyashio region of the western subarctic Pacific every one to three months from May 2002 to December 2007. The total number of samples was 56 (Table 1). The twin NORPAC nets were equipped with a flow-meter (Rigosha Co. Ltd.) in their mouths to register the volume of water filtered. The filtration efficiency of the net was $99.4 \pm 2.2\%$ (mean $\pm$ 1 sd) for the 0.335 mm mesh and $90.7 \pm 3.6\%$ for the 0.100 mm mesh. Because both nets had the same mouth diameter, some of the larger animals may have been excluded by both nets in this study. Samples were preserved on board in 5% borax-buffered formalin in seawater. Temperature and salinity data were obtained with a CTD system (Sea-Bird SBE-911 Plus).

Table 1
Zooplankton sampling dates at Site H in the Oyashio region, western subarctic Pacific during 2002–2007.

2002/2003		2004/2005		2006/2007	
Date	Day of year	Date	Day of year	Date	Day of year
18 May 02	139	7 Feb. 04	39	10 Mar. 06	70
6 June 02	158	9 Mar. 04	70	11 Mar. 06	71
12 July 02	194	13 Mar. 04	74	9 May 06	130
12 Aug. 02	225	15 Mar. 04	76	18 May 06	139
8 Oct. 02	282	9 May 04	131	23 May 06	144
17 Dec. 02	352	1 June 04	154	2 June 06	154
11 Feb. 03	42	11 June 04	164	29 July 06	181
11 Mar. 03	71	25 June 04	178	25 Oct. 06	299
10 May 03	131	21 Aug. 04	235	26 Oct. 06	300
20 May 03	141	4 Sep. 04	249	27 Oct. 06	301
3 June 03	155	5 Sep. 04	250	14 Dec. 06	349
14 June 03	166	14 Dec. 04	349	15 Dec. 06	350
27 June 03	179	15 Dec. 04	350	8 May 07	129
22 Aug. 03	235	19 Mar. 05	79	18 May 07	139
4 Oct. 03	278	10 May 05	131	1 July 07	183
16 Dec. 03	351	21 May 05	142	25 Aug. 07	238
		29 May 05	150	10 Dec. 07	345
		3 June 05	155	11 Dec. 07	346
		13 June 05	165		
		27 June 05	179		
		22 Aug. 05	235		
		14 Dec. 05	349		

2.2. OPC measurement

For optical analysis, a laboratory OPC (Model OPC-1L, Focal Technologies Inc.) with a 2×2 cm^2 opening and a 4-mm-thick beam, developed to sense zooplankton flow through the system

(Herman, 1988), was utilised in this study. To measure the sizes of the dominant copepods, we performed an OPC analysis on 30 individuals of each copepodid stage of *Neocalanus cristatus*, *Neocalanus flemingeri*, *Neocalanus plumchrus*, *E. bungii* and *M. pacifica* sorted from the formalin-preserved samples collected in the Oyashio region. The prosome length (PL) of each copepodid stage was also measured under a dissecting microscope to the nearest 0.03–0.10 mm, depending on the stage.

OPC measurements were made on samples collected by a 0.335-mm mesh size twin NORPAC net (0–150 m and 0–500 m) (Table 1). Zooplankton samples were split (Motoda, 1959), and half of the aliquots were filtered on 0.100-mm mesh under low vacuum and then weighed (wet mass: WM) to a precision of 0.01 g (Mettler PM4000). Subsamples (1/2–1/16) of the remaining aliquots were used for OPC measurements. Procedures for OPC measurements followed those of Yokoi et al. (2008); thus, (1) the flow rate of samples was approximately 10 L min^{-1}, (2) zooplankton counts were kept to less than 10 counts s^{-1} and (3) counts were performed once without staining to avoid damage to the specimens. This flow rate is substantially lower than that of any other study using the same laboratory OPC-1L (25 L min^{-1}, Moore and Suthers, 2006).

2.3. Microscopic analysis

In the Oyashio region, large copepods (*N. cristatus*, *N. flemingeri*, *N. plumchrus*, *E. bungii* and *M. pacifica*) are known to dominate the mesozooplankton biomass (73% of annual mean (Ikeda et al., 2008)). To evaluate growth across the whole population, we examined samples from 0 to 500 m collected with 0.100-mm mesh. For collection efficiency between the 0.335 mm and 0.100 mm mesh nets, stages C1–C6 of *E. bungii* and *Neocalanus* spp. were all quantitatively collected by both nets, whereas C1–C3 of *M. pacifica* were not quantitatively collected with the 0.335 mm mesh (Yamaguchi et al., 2010). We counted each copepodid stage of the five species listed above based on subsamples (1/1–1/40, made with a wide-bore pipette). We multiplied the individual dry mass of each stage (Ueda et al., 2008) by the abundance of that stage counted in each sample.

2.4. OPC data processing

2.4.1. Abundance

Based on the OPC data, the zooplankton abundance was calculated within each of 4096 equivalent spherical diameters (ESD, mm) as follows:

$$N = \frac{n}{sF} \quad (1)$$

where N is the abundance (N: ind. m^{-3}), n is the counted number, s is the subsample factor and F is the volume of water filtered through net towing (m^3). From the abundance data (N), we calculated standing stocks (ind. m^{-2}, 0–150 or 0–500 m) by multiplying by the maximum depth (150 or 500 m).

2.4.2. Biomass

Based on OPC-derived ESD data (mm), the biovolume (mm^3) of zooplankton within each 4096 ESD size unit was calculated (i.e., biovolume $= 4/3\pi[ESD/2]^3$). The wet mass (mg WM) of each size class was calculated from the biovolume of a size-specific particle, assuming the specific gravity of zooplankton to be equal to that of water (e.g., 1 mg WM = 1 mm^3). Assuming the water content of zooplankton to be 90% (cf. Yamaguchi et al., 2005), DM was calculated (DM = 0.1WM). Thus, the obtained DM conversion factor of each 4096 ESD size unit (g DM ind.$^{-1}$) was multiplied by the abundance (ind. m^{-3} or ind. m^{-2}) to obtain the total DM (g DM m^{-3} or g DM m^{-2}).

2.5. Analysis of seasonal sequence

We constructed seasonal changes for each parameter based on data from multiple years (cf. Miller and Terazaki, 1989; Osgood and Frost, 1994). The procedures used were based on those of Osgood and Frost (1994), who evaluated the life cycles of three copepods in Dabob Bay, Washington based on assemblage data that were constructed from data from multiple years (1973, 1982 and 1983).

Integrated mean temperature and salinity in the 0–150 m depth stratum were calculated for each sampling date. The data were arranged in order of Julian day (365 days) without reference to year. Data between the sampling dates were linearly interpolated at intervals of 15 days. For each parameter, data were smoothed by applying a 30-day moving average.

The abundance and biomass estimates derived from the OPC analysis were summed into six ESD size classes (<0.5, 0.5–1.0, 1.0–2.0, 2.0–3.0, 3.0–4.0 and >4.0 mm). For each size class, a seasonal time series was obtained via the same method applied to the environmental parameters. The abundance and biomass in ind. m^{-2} and g DM m^{-2}, respectively, in the 150–500 m stratum were calculated by subtracting the 0–150 m values from the 0 to 500 m values. This depth-subtraction step, called the "subtracting method", has not been used recently; however, this method of estimating the abundance of zooplankton in a discrete depth interval (without the use of an opening/closing net) was used >50 years ago (Motoda and Anraku, 1954, 1955). For the abundance and biomass of large copepods obtained by microscopic analysis, data were standardised with the procedures mentioned above.

3. Results

3.1. OPC calibration and dominant copepods

There was a highly significant correlation between the OPC-derived ESD (Y) and PL (X) of copepods: $Y = 0.478\ X$ ($r^2 = 0.96$, $p < 0.0001$, Fig. 2a). For total WM, there was a highly significant correlation between OPC-derived WM (Y') and directly measured WM (X'): $Y' = 0.934X'$ ($r^2 = 0.67$, $p < 0.0001$). Because the conversion factor (0.934) was slightly lower than 1, the OPC measurement slightly underestimated the directly measured values (Fig. 2b). The ESD size classes of each copepodid stage of dominant copepod species are shown in Table 2. Based on our six composite ESD size classes (<0.5, 0.5–1.0, 1–2, 2–3, 3–4 and >4.0 mm), the copepodid ESD sizes of the dominant copepod species were <0.5, 0.5–1.0, 1–2, 2–3 and 3–4 mm. Because the ESDs of dominant copepods were smaller than 4.0 mm, the size class >4.0 mm was thought to consist of the large zooplankton (e.g., chaetognaths, salps and euphausiids).

3.2. Seasonal changes in hydrography

The integrated temperature in the 0–150 m stratum of the water column varied between 2.9 °C in March and 11.0 °C in November (Fig. 3a). The temperature peaked in November, decreased until March, gradually increased until September, and then rapidly increased from September to November. The integrated mean salinity in the 0–150 m stratum varied between 33.16 in September and 33.75 in November. The high-salinity season (November) corresponded to the peak temperature (Fig. 3a). In terms of the water masses, the low-temperature and less saline Oyashio water dominated from January to September, whereas the higher-temperature and saline water was observed in November; a mixture of these two waters was observed in October and December (Fig. 3b).

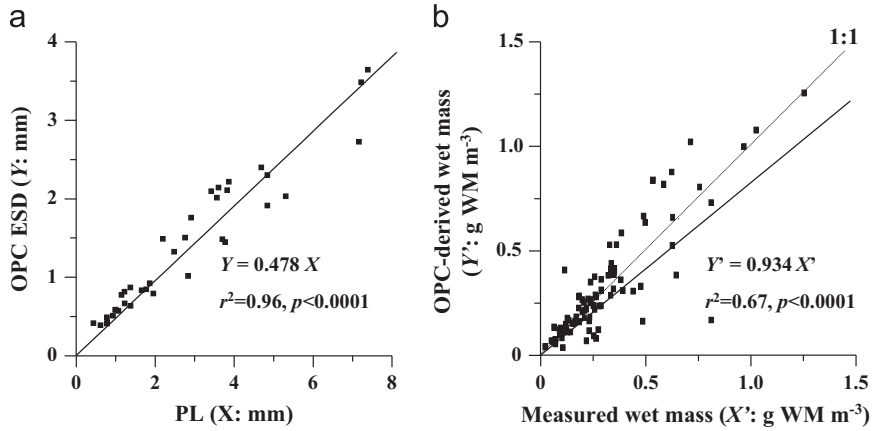

Fig. 2. Relationship between the OPC-derived ESD and prosome length (PL) of copepods (a) and between OPC-derived wet mass and directly measured wet mass (b).

Table 2
Equivalent spherical diameter (ESD) size class of each copepodid stage of the dominant calanoid copepods in the Oyashio region. Mean ESD values are shown with ±1 sd in the parentheses. All the measurements were done for 30 individuals of each stage. Note that the sex separation was not done for *Neocalanus* spp. because of the low abundance.

Size class (ESD: mm)	*Neocalanus cristatus*		*Neocalanus flemingeri*		*Neocalanus plumchrus*		*Eucalanus bungii*		*Metridia pacifica*	
< 0.5			C1	(0.409 ± 0.040)	C1	(0.417 ± 0.06)			C1	(0.411 ± 0.088)
									C2	(0.451 ± 0.044)
									C3	(0.490 ± 0.074)
0.5–1.0	C1	(0.509 ± 0.059)	C2	(0.667 ± 0.124)	C2	(0.569 ± 0.102)	C1	(0.635 ± 0.069)	C4F	(0.586 ± 0.071)
	C2	(0.823 ± 0.101)	C3	(0.846 ± 0.098)	C3	(0.833 ± 0.082)	C2	(0.793 ± 0.116)	C4M	(0.584 ± 0.089)
									C5F	(0.868 ± 0.100)
									C5M	(0.774 ± 0.088)
									C6M	(0.814 ± 0.132)
1.0–2.0	C3	(1.504 ± 0.225)	C4	(1.324 ± 0.191)	C4	(1.76 ± 0.140)	C3	(1.016 ± 0.102)	C6F	(1.489 ± 0.175)
							C4F	(1.447 ± 0.182)		
							C4M	(1.483 ± 0.162)		
							C5M	(1.916 ± 0.180)		
2.0–3.0	C4	(2.399 ± 0.456)	C5	(2.013 ± 0.255)	C5	(2.109 ± 0.292)	C5F	(2.031 ± 0.285)		
			C6	(2.097 ± 0.591)	C6	(2.141 ± 0.079)	C6F	(2.728 ± 0.416)		
							C6M	(2.303 ± 0.199)		
3.0–4.0	C5	(3.643 ± 0.368)								
	C6	3.750[a]								

[a] C6 of *N. cristatus* was estimated from the prosome length ratio between C6 and C5 reported by Kobari and Ikeda (1999).

3.3. Seasonal changes in zooplankton (OPC analysis)

The zooplankton abundance peaked in June in the 0–150 m stratum and in August for the deeper stratum (150–500 m) (Fig. 4a and b). The abundance peak at 0–150 m was 138,000 ind. m^{-2}, and the < 0.5-mm and 0.5–1.0-mm size classes predominated (ca. 80% of total zooplankton, Fig. 4a). The abundance peak at 150–500 m was lower (105,000 ind. m^{-2}) than that for 0–150 m (Fig. 4b). The contribution to abundance from the < 0.5-mm size class was lower than those of the 0.5–1.0-mm and 1.0–2.0-mm size classes for the 150–500 m stratum.

Zooplankton biomass also peaked in June for the shallower stratum (0–150 m, 10.7 g DM m^{-2}) and in August for the deeper stratum (150–500 m, 14.4 g DM m^{-2}) (Fig. 4c and d). These biomass peak seasons corresponded to the peaks in abundance. The peak biomass values for the 150–500 m stratum were greater than those for 0–150 m. This depth pattern of biomass was opposed to that of abundance. For biomass, the contribution of the smaller size classes was smaller than that of larger ones.

The seasonal changes in biomass of each size class at each depth are shown in Fig. 5. The peak in total biomass at 0–150 m was in June (Fig. 4c), and the size classes that peaked in the same period were < 0.5, 1.0–2.0 and 2.0–3.0 mm (Fig. 5a, c, and d). For the 150–500 m stratum, the total biomass peaked in August (Fig. 4d), and the size classes of 0.5–1.0, 2.0–3.0, 3.0–4.0 and > 4.0 mm had peaks in that period (Fig. 5b and d–f). Based on their dominant contributions to biomass and similar seasonal patterns, the seasonal sequences of both depth strata were driven primarily by the size classes of 1.0–2.0 and 2.0–3.0 mm.

3.4. Seasonal changes in dominant copepods (microscopic analysis)

The seasonal changes in abundance and biomass, as well as the corresponding stage compositions of dominant copepod species at 0–500 m, are shown in Figs. 6 and 7. The abundance of *N. cristatus* was greater in February (6680 ind. m^{-2}) and lower from July to November (ca. 1500 ind. m^{-2}, Fig. 6a). The abundance of *N. cristatus* C1 peaked from December to January (64%), developed through C2–C4, and then reached C5 between April and July. The mean biomass of *N. cristatus* was greater from April to August (1.2–1.9 g DM m^{-2}), and C5 predominated in biomass throughout the year. C6 individuals were very rare above 500 m.

The abundance of *N. flemingeri* peaked at 8566 ind. m^{-2} in March, and dropped to scarcity (approximately 900 ind. m^{-2})

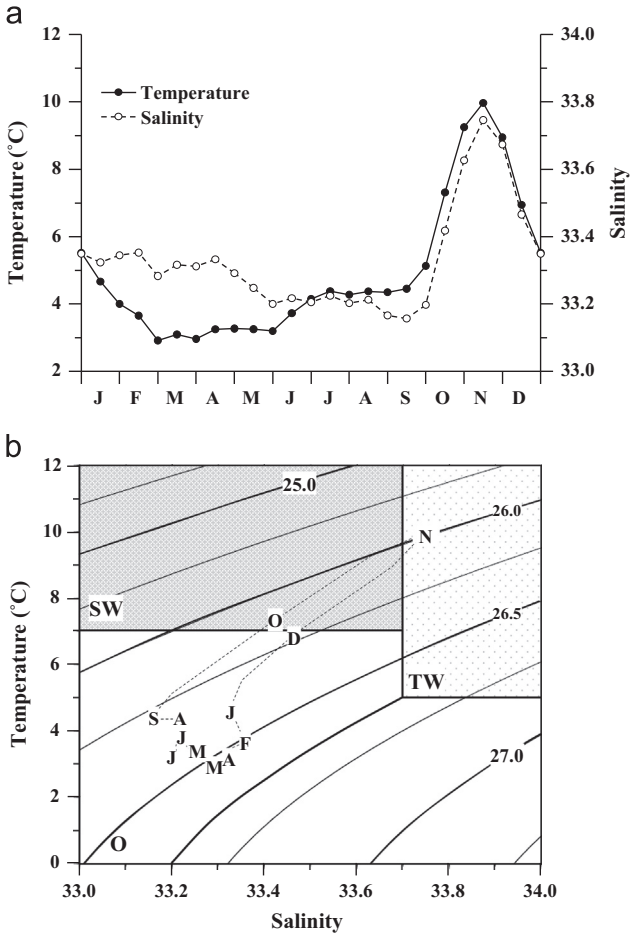

Fig. 3. Temporal changes in integrated mean temperature and salinity in the 0–150 m water column in the Oyashio region (a). Values are means of 2002–2007. Temporal changes in the *T–S* diagram of integrated mean values for the 0–150 m water column (b). Values in panel (b) indicate sigma-T (density). Classification of water masses (Hanawa and Mitsudera, 1987) is also shown in (b). O: Oyashio Water, SW: Surface-layer water and TW: Tsugaru Warm Water.

from July to December (Fig. 6b). Early copepodid stages predominated in March (C1–C3 comprised 66% of total). This population developed to C5 in June and C6 in July. The biomass of *N. flemingeri* exhibited a sharp peak from May to June (1.5 g DM m^{-2}), and C5 and C6 dominated the biomass at that period (80–100%). During January to April, the composition of C4 was also high (ca. 40%).

The maximum abundance of *N. plumchrus* reached 12,349 ind. m^{-2} from April to July, and the abundance of stage C1 peaked in May (Fig. 6c). This newly recruited population developed through C2–C4, reaching C5 in July. The biomass of *N. plumchrus* reached a sharp peak in July, and C4 and C5 were the predominant stages, while their dominant period varied seasonally: December–March for C4 and May–October for C5.

The abundance of *E. bungii* varied from 2746 to 26,929 ind. m^{-2} and was greatest from June to August (Fig. 7a). C1 and C2 were only observed from April to August, whereas C3–C6 predominated during the rest of the year. The abundance of C6 was highest in February for males and in April for females, which was one to two months earlier than the peak of C1 abundance. The biomass peak of *E. bungii* was 3.0 g DM m^{-2} in May, earlier than the peak for abundance (June–August). Late copepodid stages such as C5 and C6 were the major component of the *E. bungii* biomass.

The abundance of *Metridia pacifica* varied from 10,180 ind. m^{-2} in February to 54,056 ind. m^{-2} in June and was highest from May to July (Fig. 7b). Early copepodid stages such as C1–C3 were abundant from May to July. The biomass of *M. pacifica* peaked in April (2.9 g DM m^{-2}) and was composed primarily of C6, whereas the ratio of C5 to C6 increased in June–August.

4. Discussion

4.1. OPC calibration

There are several possibilities for under- or overestimation of sizes or numbers of particles by the OPC. Contributions from detritus and large phytoplankton to OPC data are inevitable for in-situ OPC (OPC-2T). However, for laboratory use of an OPC (OPC-1 L) as in this study, those factors (detritus and large phytoplankton) were eliminated by excluding samples dominated by detritus and large phytoplankton from the analyses (cf. Moore and Suthers, 2006). Underestimation of numbers can be caused by coincidences of particles, and underestimation of size can occur as a result of the transparent bodies of some zooplankters (Herman, 1992; Sprules et al., 1998; Zhang et al., 2000). Overestimation of body sizes can be caused by coincidences of particles, and overestimation of numbers can be caused by the presence of detritus and fragments of damaged specimens (Sprules et al., 1998; Beaulieu et al., 1999; Zhang et al., 2000). For the measurement of preserved samples, shrinkage of body sizes in gelatinous zooplankton causing underestimation of sizes and reduction of body transparency in copepods causing overestimation of sizes have been reported as sources of error in OPC measurements (Beaulieu et al., 1999).

In the present study, samples were omitted if phytoplankton or large salps dominated the biomass (8 of 112 samples were excluded, see plot in Fig. 2b). If we include these data, the factor changes greatly ($Y'=0.934X'$ to $Y'=0.438X'$). Samples where phytoplankton predominated had low biomass estimates from the OPC measurements. Because the OPC could only detect particles larger than 250 μm ESD, it may not adequately measure phytoplankton-dominated samples. Furthermore, the degree of underestimation is known to be large for sizes near the instrument detection limits (Herman, 1992).

A significant positive correlation was observed between OPC-derived ESD and the PL of copepods (Fig. 2a). Huntley et al. (2006) reported the relationship between copepod PL and OPC ESD off Hawaiian waters to be PL=1.9ESD. Although the location (subarctic vs. subtropical) and target species vary between that study and the present work, our obtained equation, PL=2.0ESD (i.e., ESD=0.478PL, Fig. 2a), is very similar to that of Huntley et al. (2006). This suggests that differences in copepod species composition have little effect on the relationship between the ESD and PL of copepods.

4.2. Hydrography

The integrated mean temperature and salinity of the 0–150 m depth range in the Oyashio region varied with season (Fig. 3a). According to the classification of water masses by Hanawa and Mitsudera (1987), the water mass in November was the Tsugaru Warm Water (Fig. 3b). Hanawa and Mitsudera (1987) also noted that the mixture of Kuroshio and Oyashio water may plot within the Tsugaru Warm Water in their *T–S* diagram. Yasuda et al. (1992) reported that warm-core rings separated from Kuroshio often move northwards to 40°N latitudes. Bearing this in mind, we considered that the water mass in November classified as the Tsugaru Warm Water in this study might also be a mixture of Kuroshio and Oyashio waters. Per the hydrographic characteristics of the Oyashio region, the variability in *T–S* diagrams from January to September was lower than that from October to December. Thus, the water mass at the 0–150 m depth range within the Oyashio region was separated into two seasons: January–September, when the water is

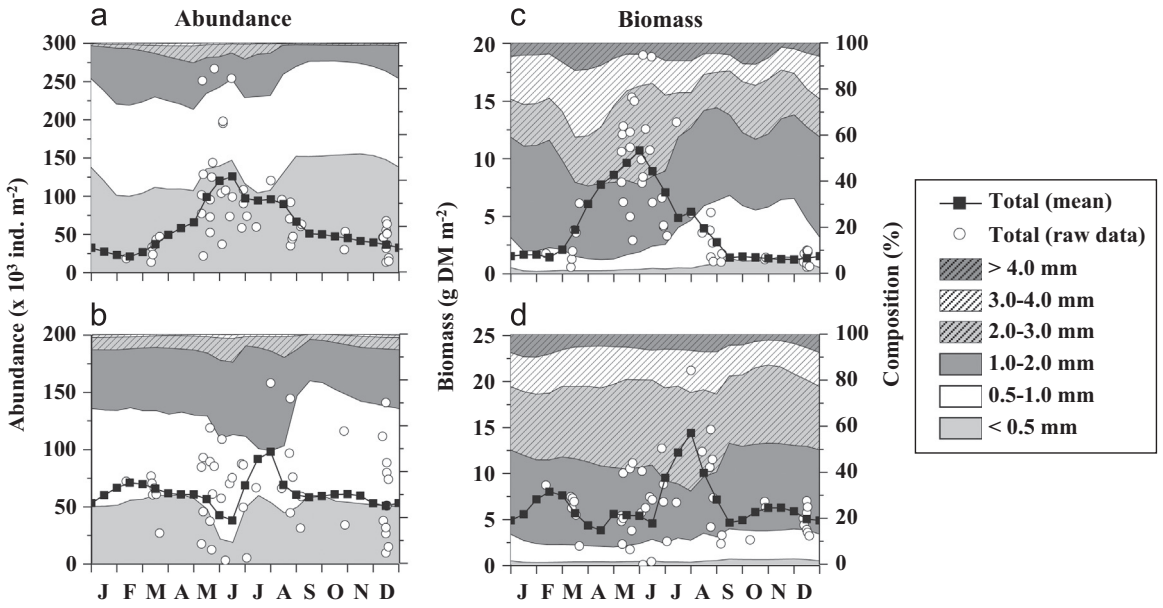

Fig. 4. Temporal changes in zooplankton size composition derived from OPC analysis: abundance in the 0–150 m (a) and 150–500 m (b) strata of the water column and biomass in the 0–150 m (c) and 150–500 m (d) strata in the Oyashio region.

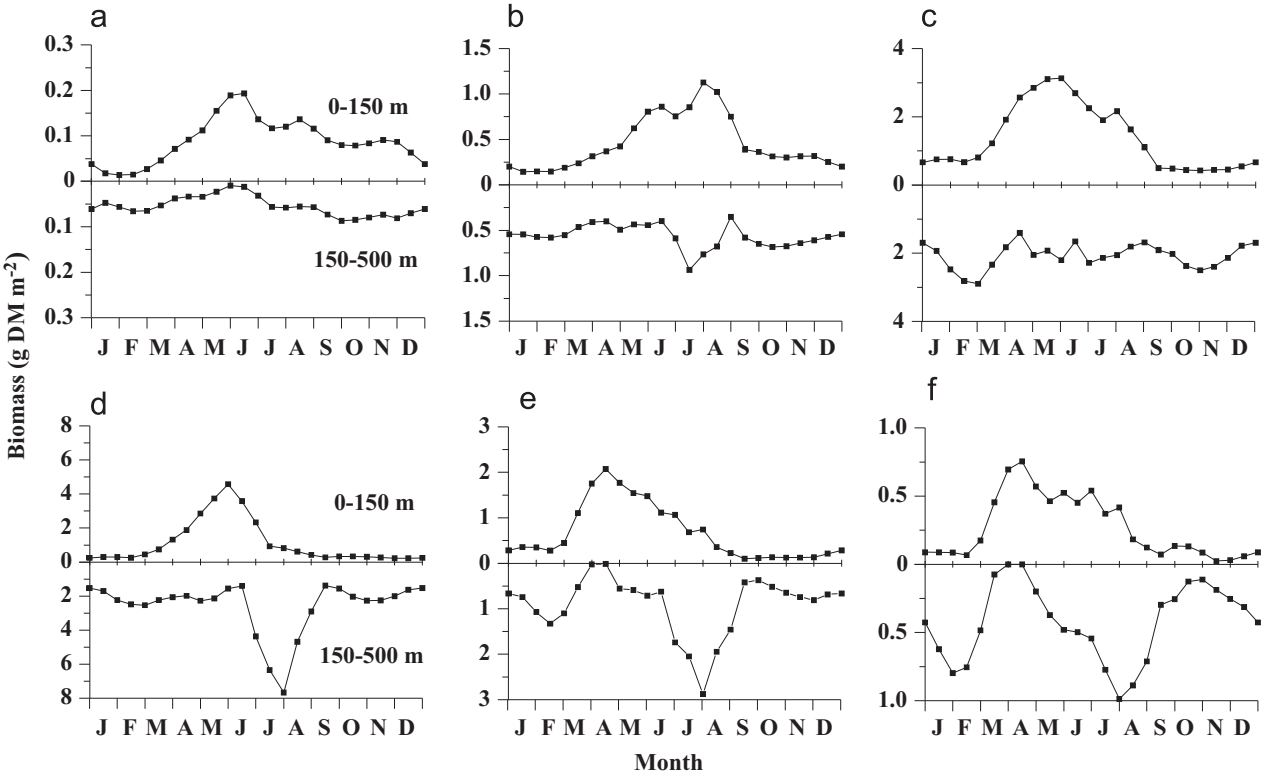

Fig. 5. Temporal changes in biomass in the 0–150 m stratum (upper panels) and the 150–500 m stratum of the water column (lower panels) in the Oyashio region for each ESD size class: <0.5 mm (a), 0.5–1.0 mm (b), 1.0–2.0 mm (c), 2.0–3.0 mm (d), 3.0–4.0 mm (e) and >4.0 mm (f), analysed by OPC measurement.

dominated by the local Oyashio water, and October–December, when the water is dominated by the mixture of Kuroshio and Oyashio waters.

4.3. Life cycle of copepods

The seasonal developmental pattern estimated by tracing the sequence of mean copepodid stages of the population at each sampling date revealed that the recruitment season of the C1 population was January for *N. cristatus*, March for *N. flemingeri* and May for *N. plumchrus* and *E. bungii*. In contrast to these copepods with single recruitment seasons per year, *M. pacifica* exhibited continuous recruitment. The phenology of reproduction and development for these copepods reflects species-specific differences in their energy utilisation patterns; *M. pacifica* and *E. bungii* spawn in the phytoplankton-rich surface layer in spring (females need to feed for

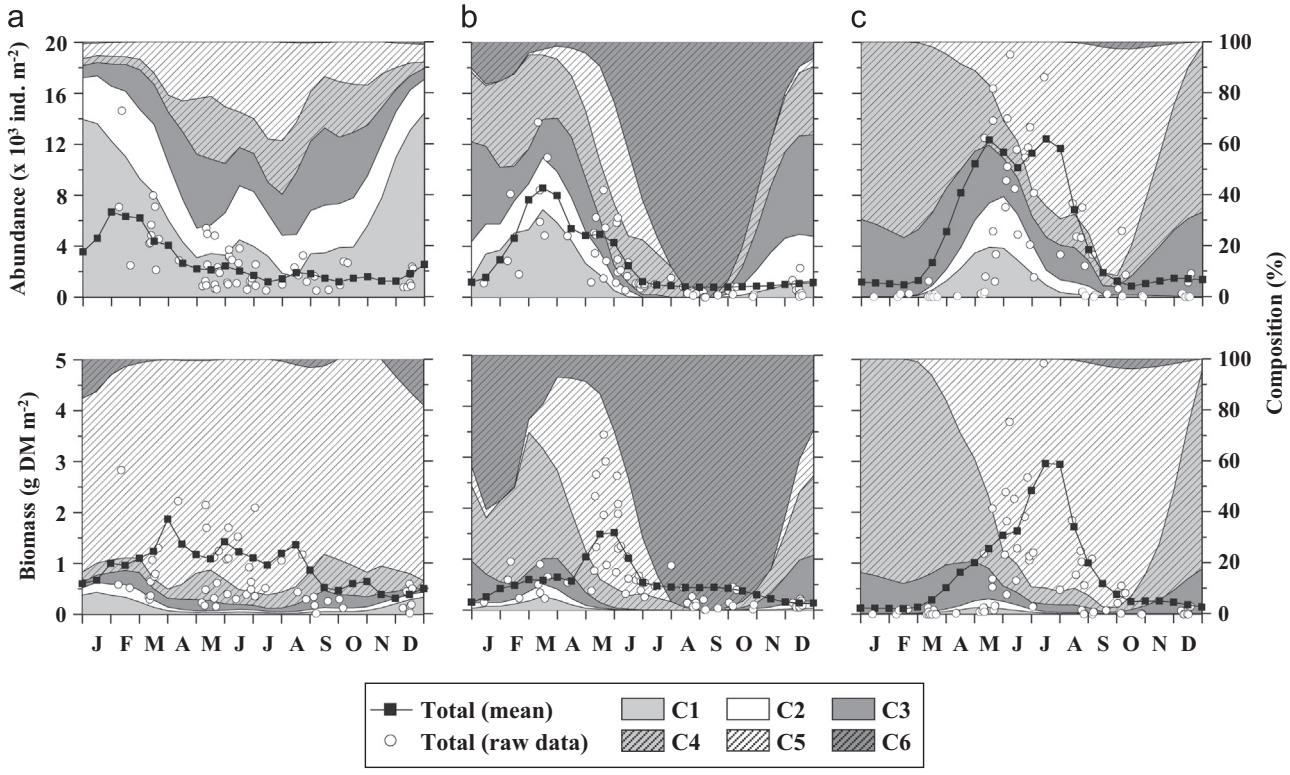

Fig. 6. Temporal changes in abundance (upper panels) and biomass (lower panels) and stage compositions of *Neocalanus cristatus* (a), *N. flemingeri* (b) and *N. plumchrus* (c) in the Oyashio region. Note that the biomass was estimated by multiplying individual mass by abundance (Ueda et al., 2008).

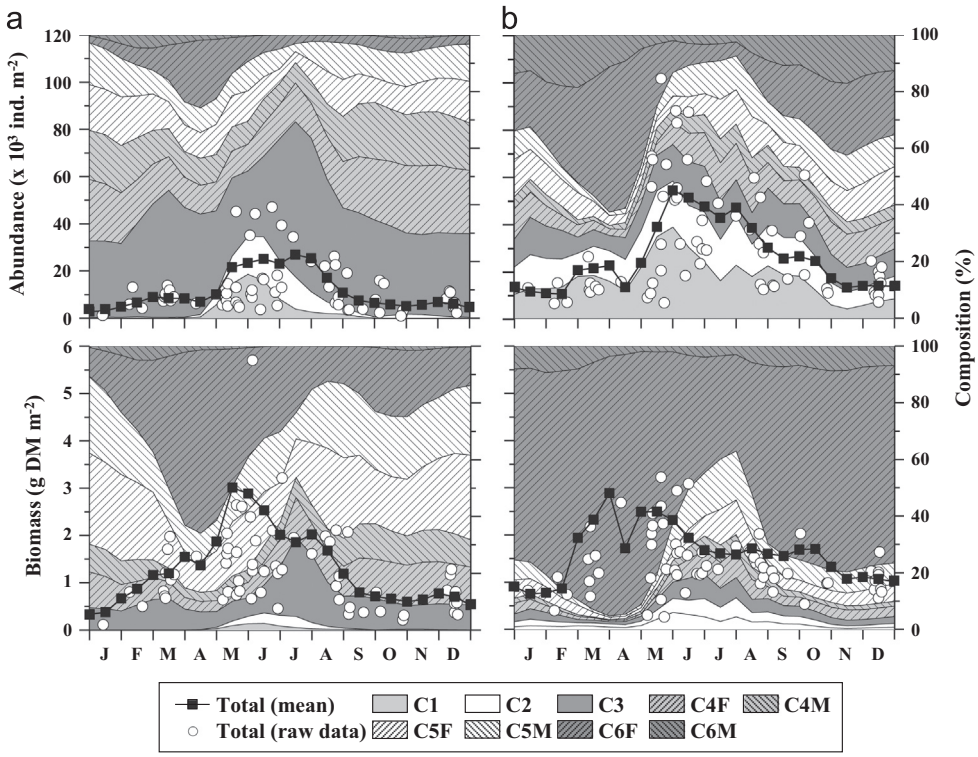

Fig. 7. Temporal changes in abundance (upper panels) and biomass (lower panels) and stage compositions of *Eucalanus bungii* (a) and *Metridia pacifica* (b) in the Oyashio region. Note that the biomass was estimated by multiplying individual mass by abundance (Ueda et al., 2008).

spawning), whereas *Neocalanus* spp. spawn in deeper water in winter (females do not feed). The development from C1 to C5 of *N. cristatus*, *N. flemingeri* and *N. plumchrus* occurs from January to June, March to June and May to August, respectively; thus, the three sympatric *Neocalanus* spp. exhibited a clear temporal separation in their developmental timing in the western subarctic Pacific. This temporal separation in utilising the surface layer is considered to be a mechanism to reduce inter-specific food competition.

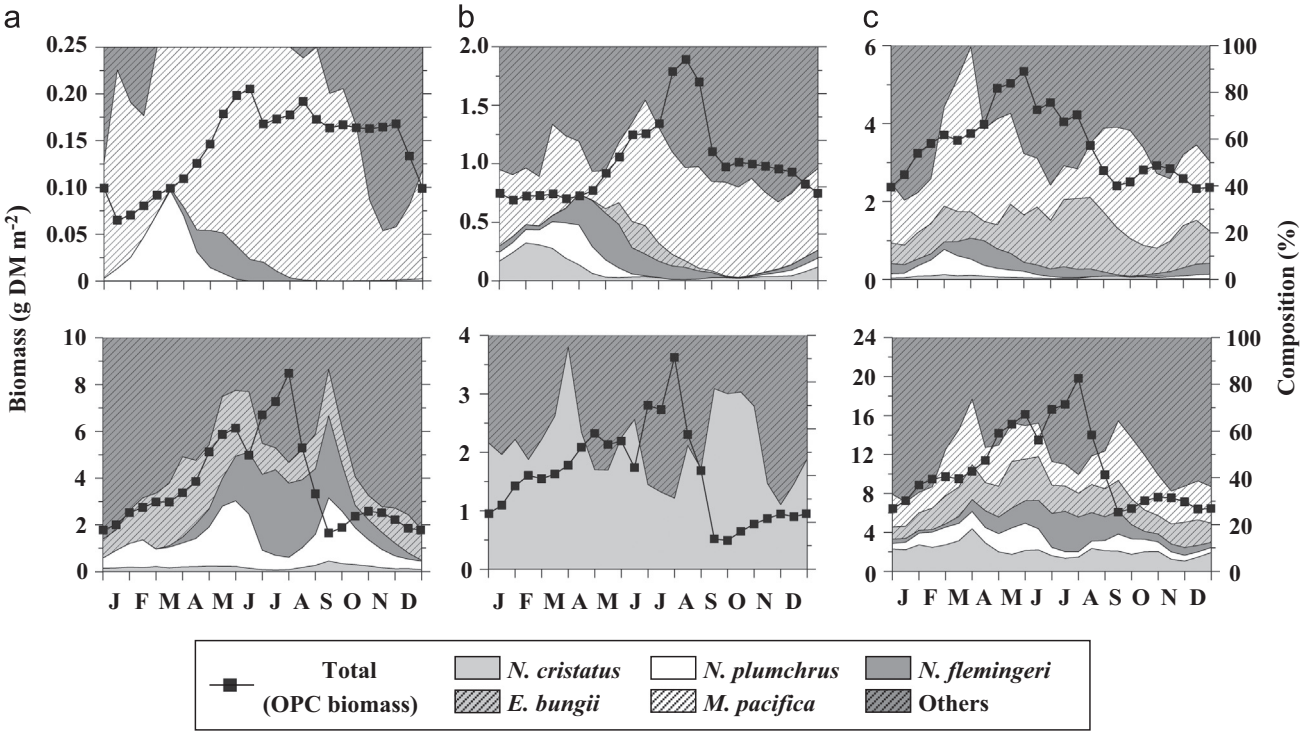

Fig. 8. Temporal changes in the species composition of dominant copepods in terms of zooplankton biomass for each size class (< 0.5 (a), 0.5–1.0 (b), 1.0–2.0 (c), 2.0–3.0 (d), 3.0–4.0 mm (e) and Total (f)) in the 0–500 m water column of the Oyashio region, derived from microscopic analysis (Figs. 6 and 7) and OPC analysis (Fig. 4). Note that the biomass of "Others" is calculated as the difference ([OPC derived mass] – [Microscopic derived copepod mass]).

The copepod abundance peaks measured here all corresponded with the peak period of recruitment of the early copepodid stage of each species. Their biomass peaks corresponded with the seasons when the majority of each population reached the late copepodid stages (Figs. 6 and 7). Interestingly, the order of the abundance and biomass peaks varied with species. For *Neocalanus* spp., the biomass peaks were observed after the abundance peaks. In contrast, the biomass peaks of *E. bungii* and *M. pacifica* were observed well before the abundance peaks. The species-specific differences in the sequence of the abundance and biomass peaks are attributed to their ontogenetic vertical migrations and our maximum sampling depth. *Neocalanus* spp. are known to develop to C5 at the surface layer, then migrate down to deep layers, where they develop to C6 and reproduce without feeding. Because of this life-cycle schema, it is reasonable that their biomass peaks are observed when they reach C5, after the abundance peak (recruitment of juvenile stages) at the surface layer (Fig. 6). In contrast to *Neocalanus* spp., reproduction in *E. bungii* and *M. pacifica* is performed by overwintered specimens at the surface layer, and their biomass peaks thus correspond to the peak of C6F, which occurs earlier than the abundance peaks (composed of the subsequent juvenile stages) (Fig. 7). Hence, the species-specific differences in the sequence of the abundance and biomass peaks are based on species' life-cycle patterns, the study's maximum sampling depth, and our seasonal reference (January–December).

4.4. Seasonal changes in zooplankton size composition

To clarify which species had the greatest influences on the seasonal changes in the biomass of each size class, we combined stage-specific size-class data (Table 2) with seasonal changes in stage-specific biomass data for the 0–500 m depth range (Figs. 6 and 7) and then added the seasonal biomass data for 0–500 m derived from OPC (Fig. 8). In this calculation, the remaining fraction is regarded as "Others" (Fig. 8). Differences in mesh size between the OPC (0.335 mm) and microscopic (0.100 mm) analyses had little effect on the results in terms of biomass. All of the copepodid stages (C1–C6) of *Neocalanus* spp. and *E. bungii* were quantitatively collected by both nets, whereas C1–C3 of *M. pacifica* were not quantitatively collected by the 0.335 mm mesh (Yamaguchi et al., 2010). However, the copepod biomass was dominated by the middle to late copepodid stages (cf. Figs. 6 and 7), i.e., those stages that were quantitatively collected with both mesh sizes. We applied only biomass units to combine the OPC and microscopic data. Thus, we see little effect of the difference in mesh size on the biomass analysis.

The size classes of the late copepodid stages of *Eucalanus bungii* and *Metridia pacifica*, which reproduce in the surface stratum, were 1.0–2.0 and 2.0–3.0 mm (Table 2, Fig. 8c and d). The late copepodid stages of *Neocalanus* spp. were primarily composed of the size classes of 2.0–3.0 and 3.0–4.0 mm (Table 2, Fig. 8d and e). The biomass peak of 1.0–2.0 mm in the 0–150 m stratum was observed from May to June (Fig. 5c), corresponding to the period when *M. pacifica* dominated (Fig. 8c). The biomass peak of 2.0–3.0 mm at 0–150 m was in May (Fig. 5d), corresponding to the period when *E. bungii* dominated (Fig. 8d). For the 150–500 m stratum, a clear peak was observed in the size class of 2.0–3.0 mm in August (Fig. 5d), corresponding to the period when *N. plumchrus* dominated (Fig. 8d). From these results, it could be inferred that the biomass peak at 0–150 m was caused primarily by the two surface-spawners, *E. bungii* and *M. pacifica*, whereas the biomass peak at 150–500 m was governed mainly by the larger *Neocalanus* spp. Thus, the depth-related differences in seasonal changes in zooplankton biomass are due to the depth strata being governed by different species: *E. bungii* and *M. pacifica* for 0–150 m and *Neocalanus* spp. for 150–500 m.

The annual mean ratio of these dominant copepods to the total zooplankton in terms of biomass was approximately 48% (Fig. 8f). This composition ratio is lower than the 73% reported for the zooplankton biomass in the water column from 0 to 2000 m

(Ikeda et al., 2008). Because our estimation covers only 0–500 m, it appears to omit most of the diapausing *Neocalanus* fraction, which is known to sink below 500 m during its ontogenetic vertical migration (Kobari and Ikeda, 1999, 2001a, 2001b). The body size of pre-adult *Neocalanus* spp. stages during diapausing is large, so their contribution to the total zooplankton biomass may increase at depths greater than 500 m. For example, export flux by ontogenetic vertical migration of *Neocalanus* spp. is estimated to be approximately 92% of sinking passive carbon flux at 1000 m in the Oyashio region (Kobari et al., 2003). From other studies in the subarctic Pacific, the active particle organic carbon (POC) flux by ontogenetic vertical migrating *Neocalanus* spp. is known to be greater than the passive POC (Kobari et al., 2008).

For the smallest size class (<0.5 mm), there was one period when the microscopically estimated biomass was greater than the biomass estimated by OPC (March–July, Fig. 8a). This is partly caused by the difference in mesh sizes, which were 0.100 mm for the microscopic analysis and 0.335 mm for the OPC. Furthermore, we should consider that the OPC can only detect particles greater than 0.25 mm ESD. Because the diagonal length of 0.335 mm mesh is 0.474 mm, OPC analysis may not quantitatively evaluate the <0.5-mm size class. Nevertheless, the "Others" dominated the biomass in the <0.5-mm size class from October to December (Fig. 8a). This period (October–December) corresponded to the period when warm-core rings frequently separate from the Kuroshio Current (Fig. 3b). During October to December, the total biomass of the <0.5-mm size class remained high, whereas the abundance of *M. pacifica* exhibited a sudden decrease. In the Oyashio region, small warm-water oncaeid copepods dominate the zooplankton community of warm-core rings (Nishibe and Ikeda, 2004). Thus, the dominance of "Others" in the <0.5-mm size class during October to December might be particularly affected by a warm-core ring that separated from the Kuroshio Current.

In conclusion, the method of this study—combining OPC analysis and microscopic analysis on the same samples—is valuable. From these analyses, we can obtain both size and taxonomic information. Applying the individual size and biomass data for each copepodid stage, the composition of each size class of each species in the biomass was evaluated (Fig. 8). Such comprehensive insights into the size and species composition of the zooplankton biomass could not be obtained without this method. Recently, mesozooplankton size data obtained by OPC analysis were used for Normalised Biomass Size Spectra (NBSS) analysis (Matsuno et al., 2012; Marcolin et al., 2013). However, to concentrate on size-taxonomic analysis, we did not apply NBSS analysis in this study. In the future, NBSS analysis of seasonal zooplankton samples may be needed in the Oyashio region.

Acknowledgements

Drs. Jeffery M. Napp and Deborah K. Steinberg provided useful comments on the manuscript. We are grateful to the captain, officers, crew, cadets and scientists on board T/S *Oshoro-Maru* and R/V *Ushio-Maru* of Hokkaido University for their help in collecting zooplankton samples and hydrographical data. This study was supported by Grant-in-Aid for Scientific Research (No. 24248032) and Grant-in-Aid for Scientific Research on Innovative Areas 24110005 from the Japan Society for the Promotion of Science (JSPS).

References

Beaulieu, S.E., Mullin, M.M., Tang, V.T., Pyne, S.M., King, A.L., Twining, B.S., 1999. Using an optical plankton counter to determine the size distribution of zooplankton samples. J. Plankton Res. 21 (10), 1939–1956.

Boyd, P.W., Newton, P.P., 1999. Does planktonic community structure determine downward particulate organic carbon flux in different oceanic province? Deep-Sea Res. I 46 (1), 63–91.

Ducklow, H.W., Steinberg, D.K., Buesseler, K.O., 2001. Upper ocean carbon export and the biological pump. Oceanography 14 (4), 50–58.

Hanawa, K., Mitsudera, H., 1987. Variation of water system distribution in the Sanriku coastal area. J. Oceanogr. Soc. Jpn. 42 (6), 435–446.

Herman, A.W., 1988. Simultaneous measurement of zooplankton and light attenuance with a new optical plankton counter. Cont. Shelf Res. 8 (2), 205–221.

Herman, A.W., 1992. Design and calibration of a new optical plankton counter capable of sizing small zooplankton. Deep-Sea Res. A 39 (3–4), 395–415.

Huntley, M.E., Lopez, M.D.G., Zhou, M., Landry, M.R., 2006. Seasonal dynamics and ecosystem impact of mesozooplankton at station ALOHA based on optical plankton counter measurements. J. Geophys. Res. C 111, C05S10, http://dx.doi.org/10.1029/2005JC002892.

Ikeda, T., Shiga, N., Yamaguchi, A., 2008. Structure, biomass distribution and trophodynamics of the pelagic ecosystem in the Oyashio region, western subarctic Pacific. J. Oceanogr. 64 (3), 339–354.

Kasai, H., Saito, H., Yoshimori, A., Taguchi, S., 1997. Variability in timing and magnitude of spring bloom in the Oyashio region, the subarctic Pacific off Hokkaido. Japan. Fish. Oceanogr. 6 (2), 118–129.

Kasai, H., Saito, H., Yoshimori, A., Kashiwai, M., Taneda, T., Kusaka, A., Kawasaki, Y., Kono, T., Taguchi, S., Tsuda, A., 2001. Seasonal and interannual variations in nutrients and plankton in the Oyashio region: a summary of a 10 years observation along the A-line. Bull. Hokkaido Natl. Fish. Res. Inst. 65, 57–136.

Kobari, T., Ikeda, T., 1999. Vertical distribution, population structure and life cycle of *Neocalanus cristatus* (Copepoda: Calanoida) in the Oyashio region with notes on its regional variations. Mar. Biol. 134 (4), 683–696.

Kobari, T., Ikeda, T., 2001a. Life cycle of *Neocalanus flemingeri* (Crustacea: Copepoda) in the Oyashio region, western subarctic Pacific, with notes on its regional variations. Mar. Ecol. Prog. Ser. 209, 243–255.

Kobari, T., Ikeda, T., 2001b. Ontogenetic Vertical migration and life cycle of *Neocalanus plumchrus* (Copepoda: Calanoida) in the Oyashio region, with notes on regional variations in body size. J. Plankton Res. 23 (3), 287–302.

Kobari, T., Shinada, A., Tsuda, A., 2003. Functional roles of interzonal migrating mesozooplankton in the western subarctic pacific. Prog. Oceanogr. 57 (3–4), 279–298.

Kobari, T., Steinberg, D.K., Ueda, A., Tsuda, A., Silver, M.W., Kitamura, M., 2008. Impacts of ontogenetically migrating copepods on downward carbon flux in the western subarctic Pacific Ocean. Deep-Sea Res. II 55 (14–15), 1648–1660.

Kono, T., 1997. Modification of the Oyashio water in the Hokkaido and Tohoku area. Deep-Sea Res. I 44 (4), 669–688.

Marcolin, C.R., Schultes, S., Jackson, G.A., Lopes, R.M., 2013. Plankton and seston size spectra estimated by the LOPC and ZooScan in the Abrolhos Bank ecosystem (SE Atlantic). Cont. Shelf Res. 70 (1), 74–87.

Matsuno, K., Yamaguchi, A., Imai, I., 2012. Biomass size spectra of mesozooplankton in the Chukchi Sea during the summers of 1991/1992 and 2007/2008: an analysis using optical plankton counter data. ICES J. Mar. Sci. 69 (7), 1205–1217.

Miller, C.B., Terazaki, M., 1989. The life histories of *Neocalanus flemingeri* and *Neocalanus plumchrus* in the Sea of Japan. Bull. Plankton Soc. Jpn. 36 (1), 27–41.

Moore, S.K., Suthers, I.M., 2006. Evaluation and correction of subresolved particles by the optical plankton counter in three Australian estuaries with pristine to highly modified catchments. J. Geophys. Res. C 111, C05S04, http://dx.doi.org/10.1029/2005JC002920.

Motoda, S., 1957. North Pacific standard plankton net. Inform. Bull. Planktol. Japan 4, 13–15.

Motoda, S., 1959. Devices of simple plankton apparatus. Mem. Fac. Fish. Hokkaido Univ. 7 (1–2), 73–94.

Motoda, S., Anraku, M., 1954. Daily changes of vertical distribution of plankton animals near western entrance of the Tsugaru Strait, northern Japan. Bull. Fac. Fish. Hokkaido Univ. 5 (1), 15–19.

Motoda, S., Anraku, M., 1955. Further observation on the daily changes in amount of catches of plankton animals in vertical hauls. Bull. Fac. Fish. Hokkaido Univ. 6 (1), 15–18.

Nishibe, Y., Ikeda, T., 2004. Vertical distribution, abundance, and community structure of oncaeid copepods in the Oyashio region, western subarctic Pacific. Mar. Biol. 145 (5), 931–941.

Oozeki, Y., Watanabe, Y., Kitagawa, D., 2004. Environmental factors affecting larval growth of Pacific saury, *Cololabis saira*, in the northwestern Pacific Ocean. Fish. Oceanogr. 13 (S1), S44–S53.

Osgood, K.E., Frost, B.W., 1994. Comparative life histories of three species of planktonic calanoid copepods in Dabob Bay, Washington. Mar. Biol. 118 (4), 627–636.

Saito, H., Tsuda, A., Kasai, H., 2002. Nutrient and plankton dynamics in the Oyashio region of the western subarctic Pacific Ocean. Deep-Sea Res. II 49 (24–25), 5463–5486.

Sprules, W.G., Herman, A.W., Stockwell, J.D., 1998. Calibration of an optical plankton counter for use in fresh water. Limnol. Oceanogr. 43 (3), 726–733.

Tsuda, A., Saito, H., Kasai, H., 1999. Life history of *Neocalanus flemingeri* and *Neocalanus plumchrus* (Copepoda: Calanoida) in the western subarctic Pacific. Mar. Biol. 135 (3), 533–544.

Tsuda, A., Saito, H., Kasai, H., 2004. Life history of *Eucalanus bungii* and *Neocalanus cristatus* (Copepoda: Calanoida) in the western subarctic Pacific Ocean. Fish. Oceanogr. 13 (S1), 10–20.

Ueda, A., Kobari, T., Steinberg, D.K., 2008. Body length, weight and chemical composition of ontogenetically migrating copepods in the western subarctic gyre of the North Pacific Ocean. Bull. Plankton Soc. Jpn. 55 (2), 107–114.

van der Meeren, T., Næss, T., 1993. How does cod (*Gadus morhus*) cope with variability in feeding conditions during early larval stages? Mar. Biol. 116 (4), 637–647.

Yamaguchi, A., Watanabe, Y., Ishida, H., Harimoto, T., Maeda, M., Ishizaka, J., Ikeda, T., Takahashi, M.M., 2005. Biomass and chemical composition of net-plankton down to greater depth (0–5800 m) in the western North Pacific Ocean. Deep-Sea Res. I 52 (2), 341–353.

Yamaguchi, A., Onishi, Y., Omata, A., Kawai, M., Kaneda, M., Ikeda, T., 2010. Population structure, egg production and gut content pigment of large grazing copepods during the spring phytoplankton bloom in the Oyashio region. Deep-Sea Res. II 57 (17–18), 1679–1690.

Yamamura, O., 2004. Trophodynamics modeling of walleye Pollock (*Theragra chalcogramma*) in the Doto area, northern Japan: model description and baseline simulations. Fish. Oceanogr. 13 (S1), S138–S154.

Yasuda, I., Okuda, K., Hirai, M., 1992. Evolution of a Kuroshio warm-core ring – variability of the hydrographic structure. Deep-Sea Res. A 39 (S1), S131–S161.

Yokoi, Y., Yamaguchi, A., Ikeda, T., 2008. Regional and interannual changes in the abundance, biomass and size structure of mesozooplankton in the western North Pacific in early summer analysed using an optical plankton counter. Bull. Plankton Soc. Jpn. 55 (1), 9–24.

Zhang, X., Roman, M., Sanford, A., Adolf, H., Lascara, C., Burgett, E., 2000. Can an optical plankton counter produce reasonable estimate of zooplankton abundance and biovolume in water with high detritus? J. Plankton Res. 22 (1), 137–150.